Physica D 285 (2014) 8–17

Contents lists available at ScienceDirect

Physica D

journal homepage: www.elsevier.com/locate/physd

Binocular rivalry waves in a directionally selective neural field model

Samuel R. Carroll, Paul C. Bressloff*

Department of Mathematics, University of Utah, Salt Lake City, UT 84112, USA

HIGHLIGHTS

- First analytical study of the effects of stimulus motion on the speed of binocular rivalry waves.
- Wave speed is faster for waves propagating in same direction as the stimulus, as found in experiments.
- The type of directional symmetry breaking mechanism is sensitive to the form of slow adaptation.
- Provides a specific biological application of neural field theory.

ARTICLE INFO

Article history:
Received 22 February 2014
Received in revised form
8 July 2014
Accepted 9 July 2014
Available online 16 July 2014
Communicated by S. Coombes

Keywords:
Neural field equation
Binocular rivalry
Traveling waves
Direction selectivity

ABSTRACT

We extend a neural field model of binocular rivalry waves in the visual cortex to incorporate direction selectivity of moving stimuli. For each eye, we consider a one-dimensional network of neurons that respond maximally to a fixed orientation and speed of a grating stimulus. Recurrent connections within each one-dimensional network are taken to be excitatory and asymmetric, where the asymmetry captures the direction and speed of the moving stimuli. Connections between the two networks are taken to be inhibitory (cross-inhibition). As per previous studies, we incorporate slow adaption as a symmetry breaking mechanism that allows waves to propagate. We derive an analytical expression for traveling wave solutions of the neural field equations, as well as an implicit equation for the wave speed as a function of neurophysiological parameters, and analyze their stability. Most importantly, we show that propagation of traveling waves is faster in the direction of stimulus motion than against it, which is in agreement with previous experimental and computational studies.

1. Introduction

Many perceptual phenomena in the visual system involve wave-like propagation dynamics, including perceptual filling-in [1], migraine aura [2], expansion of illusory contours [3], and the line-motion illusion [4]. Another example that has received great attention is the wave-like propagation of perceptual dominance during binocular rivalry [5–10]. Binocular rivalry is the phenomenon where perception switches back and forth between different images presented to the two eyes. This provides a way of studying the human visual system and identifying possible neural mechanisms underlying conscious visual awareness via non-invasive psychophysical experiments [11,12].

In an experimental and computational study of rivalrous moving stimuli by Knapen et al. [13], it was shown that the propagation speed of a binocular rivalry wave depends on the direction and speed of the stimuli. In the experimental portion of their study, two annular gratings were rotated at a fixed speed in opposite directions for each eye. A low contrast image was presented to one eye (the carrier stimulus) and a high contrast image was presented to the opposite eye (the mask stimulus). Finally a temporary increase of the contrast in a localized region of the low contrast image triggered a duo of wave-like perceptual transitions in dominance from mask to carrier that propagated upward within the boundaries of the annular-shaped carrier, one in the clockwise direction and one in the counter-clockwise direction (see Fig. 1). Moreover, it was found that waves travel faster in the direction of stimulus motion than they do in the opposite direction. Knapen et al. [13] also constructed a two-layer computational model with each layer driven by a single eye. They included recurrent excitation within a layer and mutual inhibition between layers. In order to model direction selective cells, the inhibitory weights were taken to have an asymmetric spatial rate of decay, that is, the efferents from a given neuron decayed more rapidly on one side of the neuron than the other (in a one-dimensional network). It was shown how such an asymmetry was able to account for the dependence of wave speed on stimulus motion.

* Corresponding author. Tel.: +1 801 585 1633.
E-mail addresses: carroll@math.utah.edu (S.R. Carroll), bressloff@math.utah.edu (P.C. Bressloff).

http://dx.doi.org/10.1016/j.physd.2014.07.002
0167-2789/

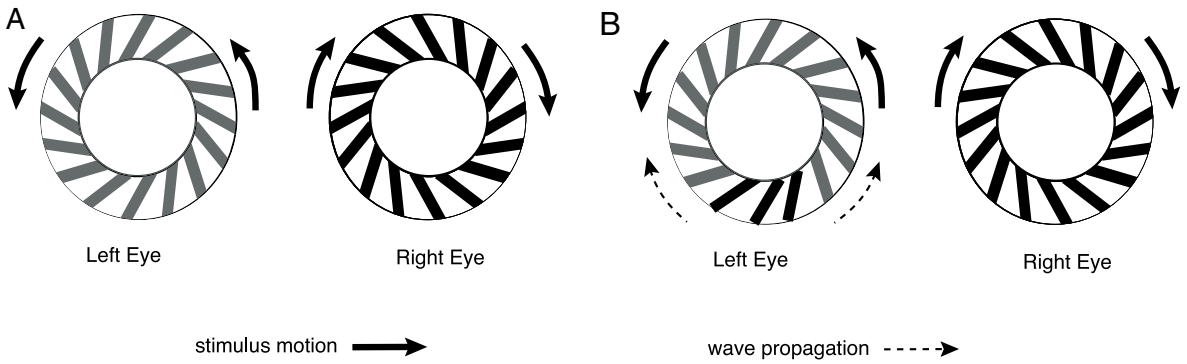

Fig. 1. Schematic illustration of rotating annuli stimuli analogous to those used by Knapen et al. [13]. A. The left (right) eye is presented with a low (high) contrast carrier (mask) stimulus rotating in an anti-clockwise (clockwise) direction. A transient increase in the contrast of the carrier stimulus induces a pair of counter propagating waves that travel from the bottom to the top of the annuli, resulting in a switch from perception of the mask to perception of the carrier. The wave traveling in the same direction as the stimulus reaches the top first, indicating that it has a higher speed.

In this paper we extend the study by Knapen et al. [13] by analyzing stimulus-motion-dependent propagation of binocular rivalry waves in a continuum neural field model. Rather than imposing an asymmetry in the spatial decay of the mutual inhibition, we shift the recurrent excitatory weight functions along the lines of previous neural field models of direction selectivity [14,15]. Such shifts were also used in earlier computational neural network models [16,17]. In the case of fully symmetric synaptic weights, we recover our previous model, which was used to analyze rivalry waves induced by switching between stationary stimuli [9,10]. In contrast to the results in Knapen et al. (2007), we find that imposing an asymmetric shift in the inhibitory weight functions yields no dependence of the wave speed on stimulus motion. Instead, we show that the asymmetric shift must occur in the recurrent weights in order to obtain motion-dependent wave speeds. We derive an analytical expression for the wave speed of both waves traveling with and against the stimulus as a function of stimulus speed, and show that the speed is greater in the direction of motion.

2. Neural field model of direction selectivity with synaptic depression

To motivate the model used in this paper, it is beneficial to first discuss the functional architecture of the primary visual cortex (V1). Each neuron in V1 responds to light stimuli in a localized region of the visual field called its classical receptive field, while stimuli outside a neuron's receptive field do not directly affect its activity. Rather, stimuli outside a neuron's receptive field will induce activity in that neuron indirectly via lateral connections with other cortical neurons. Most neurons in V1 respond preferentially to stimuli targeting either the left or right eye, which is known as ocular dominance. Experiments suggest that neurons with different ocular dominance may inhibit one another if they have nearby receptive fields [18]. Additionally, most neurons in V1 are tuned to respond maximally when a stimulus of a particular feature, such as orientation, is in their receptive field [19,20]. In the case of orientation, this is known as a neuron's orientation preference; a neuron will not respond to a stimulus with a sufficiently different orientation. It has been shown that at each point in the visual field (on an appropriately coarse-grained spatial scale), there exists a corresponding set of neurons spanning the entire spectrum of orientation preferences that are packed together as a unit in V1, known as a hypercolumn [21,22,20]. Each hypercolumn consists of neurons which, for sufficiently similar orientations, excite each other and neurons with sufficiently different orientations inhibit each other [23,24]. Anatomical evidence also suggests that inter-hypercolumn connections link neurons with similar orientation preferences [25,26]. The functional relationship between stimulus feature preferences and synaptic connections within V1 therefore suggest that V1 is a likely substrate of simple examples of binocular rivalry such as those involving sinusoidal grating stimuli [27].

A certain subset of orientation-selective neurons in V1 also respond to some directions of stimulus movement better than others [28]. For example, a neuron may respond to a vertical line moving leftwards but not moving rightwards. One mechanism for generating direction selectivity is for visual stimuli in certain parts of the receptive field to generate faster responses (shorter delays) than other regions. Given these differences in response timing, a line moving from a slow to a fast region generates a stronger response than a line moving from a fast to a slow region. That is, the delayed response in the slow region occurs at approximately the same time as the response in the fast region, resulting in a stronger total response compared to the reverse order [29]. An analogous dependence on the order of receptive field stimulation can occur if the excitatory recurrent connections within V1 are spatially shifted relative to the inhibitory connections [16,17,30]. This latter mechanism has also been incorporated into continuum neural field models of direction selectivity [14,15]; one advantage of neural field models compared to spatially discrete computational models is that the former allows analytical expressions for the stimulus–response properties of the network to be obtained [31].

Recently, we constructed a neural field model of binocular rivalry waves in the case of stationary stimuli [9]. The model consists of a one-dimensional neural field for each eye, whose dynamics represents the activity of neurons within a hypercolumn that respond maximally to the given stimulus orientation. Recurrent connections within each one-dimensional network are assumed to be excitatory, whereas connections between the two networks are taken to be inhibitory (cross-inhibition). Slow adaptation is incorporated into the model by taking the network connections to exhibit synaptic depression along the lines of Kilpatrick and Bressloff [32], see also [33]. One of the main results of our previous analysis was to show that some form of slow adaptation such as synaptic depression is required as a symmetry breaking mechanism in order to allow for the propagation of binocular rivalry waves [9]. Note that one alternative to synaptic depression is spike frequency adaptation, which has been used in a variety of other spatial and non-spatial models of binocular rivalry [5,34,35,13,8]. In this paper, we extend our previous neural field model of binocular rivalry waves, by incorporating an asymmetric shift in the recurrent connections along the lines of Refs. [14,15]. The sign and size of the shift determines the stimulus direction and speed preferences of the neurons. A schematic illustration of the network architecture is shown in Fig. 2. Following our previous work [9] and the computational model of Knapen et al. [13], we replace the more

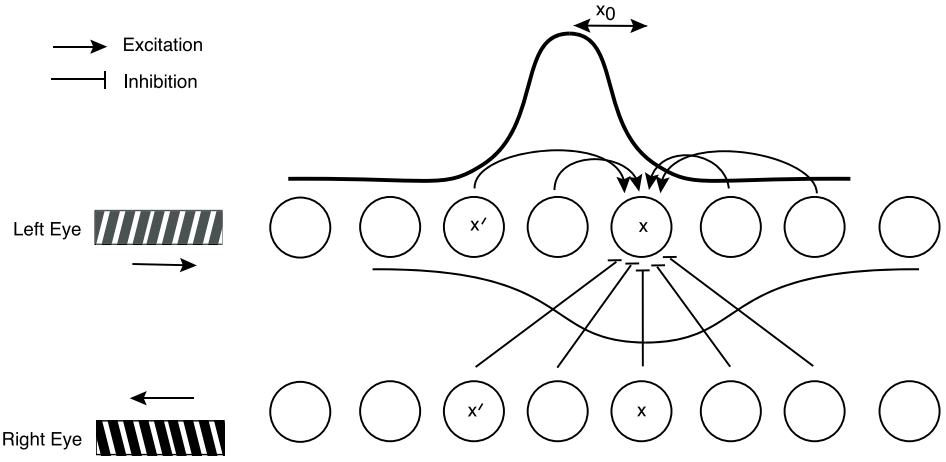

Fig. 2. Schematic diagram of network architecture consisting of two one-dimensional neural fields. The left eye is shown an oriented grating moving rightwards and the right eye is shown a different oriented grating moving leftwards. The neural fields represent the activity of neurons that respond maximally to the orientation and motion of the corresponding grating. Recurrent connections within each one-dimensional network are assumed to be excitatory, whereas connections between the two networks are inhibitory (cross-inhibition). The excitatory and inhibitory weight distributions are taken to be Gaussians with the former having an asymmetric shift of size x_0 in the left network and a shift of $-x_0$ in the right network. For the sake of illustration, the weight distributions of afferents into neurons at x are shown for the left eye network; the peak of the shift distribution occurs at $x - x_0$. Finally, slow adaptation is incorporated into the model by taking the network connections to exhibit synaptic depression.

complicated annuli stimuli by linear oriented gratings. Stationary linear gratings were also used in the psychophysical experiments of Kang et al. [7,8]. In order to consider the difference between waves moving in the same direction as the stimulus motion and waves moving in the opposite direction, we imagine inducing the switch from mask to carrier using a local change of contrast at either one end or the other of the carrier stimulus, see Fig. 3.

Let $u(x,t)$ and $v(x,t)$ denote the activity of the left and right eye networks, respectively, at position $x \in \mathbb{R}$ at time t. Then the associated neural field equation is given by

$$\begin{aligned}\tau \frac{\partial u(x,t)}{\partial t} &= -u(x,t) + I_u \\ &\quad + \int_{-\infty}^{\infty} w_{e+}(x-x')q_u(x',t)f(u(x',t))dx' \\ &\quad - \int_{-\infty}^{\infty} w_i(x-x')q_v(x',t)f(v(x',t))dx', \end{aligned} \tag{2.1a}$$

$$\tau_s \frac{\partial q_u(x,t)}{\partial t} = 1 - q_u(x,t) - \beta q_u(x,t) f(u(x,t)), \tag{2.1b}$$

and

$$\begin{aligned}\tau \frac{\partial v(x,t)}{\partial t} &= -v(x,t) + I_v \\ &\quad + \int_{-\infty}^{\infty} w_{e-}(x-x')q_v(x',t)f(v(x',t))dx' \\ &\quad - \int_{-\infty}^{\infty} w_i(x-x')q_u(x',t)f(u(x',t))dx', \end{aligned} \tag{2.2a}$$

$$\tau_s \frac{\partial q_v(x,t)}{\partial t} = 1 - q_v(x,t) - \beta q_v(x,t) f(v(x,t)). \tag{2.2b}$$

The nonlinear function f represents the mean firing rate of a local population and is usually taken to be a smooth, bounded monotonic function such as a sigmoid

$$f(u) = \frac{1}{1+e^{-\eta(u-\kappa)}}, \tag{2.3}$$

where η denotes the gain and κ the threshold. However, in order to derive explicit traveling wave solutions, it is convenient to consider the high gain limit, $\eta \to \infty$, so that f becomes a Heaviside function

$$f(u) = H(u-\kappa) = \begin{cases} 0, & \text{if } u < \kappa \\ 1, & \text{if } u > \kappa. \end{cases} \tag{2.4}$$

The functions $w_{e\pm}(x-x')$ represent the distribution of recurrent synaptic weights from the local population at x' to the population at x within the same eye network, with $(\pm)$ denoting the left and right eyes, respectively. Typically, these are taken to be symmetric functions such that $w_{e\pm}(x) = w_{e\pm}(-x)$. However, in this paper we will consider asymmetric recurrent weights of the form

$$w_{e\pm}(x) = w_e(x \mp x_0), \tag{2.5}$$

where the sign and size of the shift x_0 determines the stimulus direction and speed preferences of neurons. Hence, the shift of the left and right eye networks has the opposite sign, since they are responding to stimuli moving in opposite directions. The excitatory distribution w_e is assumed to have the following properties:

(i) $w_e \in C(\mathbb{R}) \cap L^1(\mathbb{R})$ and $dw_e/dx \in L^1(\mathbb{R})$,
(ii) $w_e(x) > 0\ \forall x \in \mathbb{R}$,
(iii) $w_e(x) = w_e(-x)$ and $w(x)$ is a monotonically decreasing function of x for $x \geq 0$.

One typically takes w_e to be a Gaussian function or an exponential function. In the latter case,

$$w_{e\pm}(x) = a_e e^{-\sigma_e|x \mp x_0|}. \tag{2.6}$$

For numerical calculations we will use Eq. (2.6). Rather than modeling the inputs I_u and I_v as depending on space and time, we simply choose the subset of neurons in V1 that respond maximally to a stimulus with a fixed speed, which is captured by the parameter x_0. For cross-inhibition we use a symmetric weight function, w_i, that satisfies properties (i)–(iii). Again, one normally defines w_i as an exponential or Gaussian. Later we will show why imposing asymmetry in the inhibition does not lead to motion dependent wave speeds. Depressing synapses are incorporated into the model in the form of presynaptic scaling factors q_u, q_v with corresponding time constant τ_s.

3. Existence of traveling waves

We now look for rivalry wave solutions in which the high activity state invades the suppressed left eye network, while retreating from the dominant right eye network. In doing so, we seek solutions of the form $u(x,t) = U(\xi)$ and $v(x,t) = V(\xi)$ where $\xi = x - ct$ and c denotes the wave speed. That is, the fixed wave profiles, $U(\xi)$ and $V(\xi)$, propagate with a speed c. Since we are

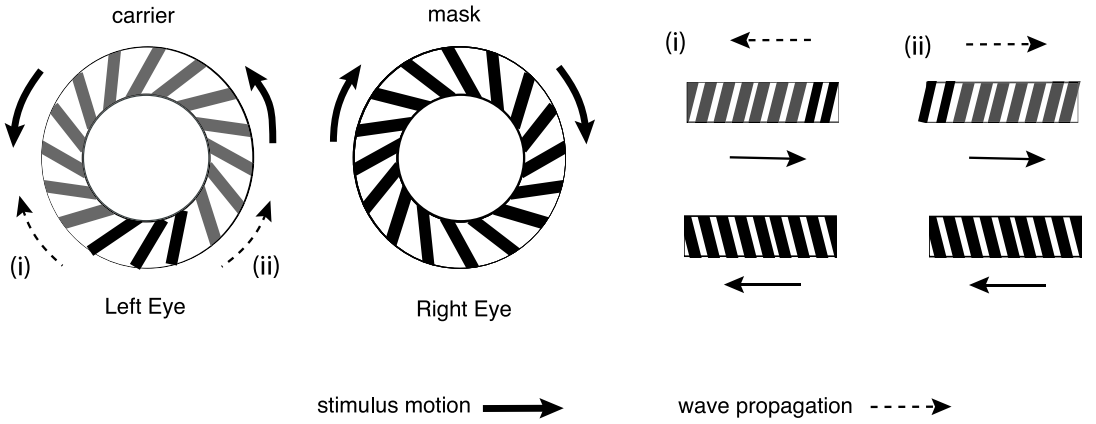

Fig. 3. Induction of a wave moving in (i) the opposite direction to stimulus motions and (ii) the same direction as stimulus motion. For annuli stimuli a local increase in the contrast of the carrier can induce both waves, whereas for linear gratings the local increase in contrast has to be induced separately at either one end or the other of the stimulus.

considering the case where high activity states invade the suppressed left eye network, we let $\lim_{\xi\to-\infty}(U(\xi), V(\xi)) = \mathbf{X}_L$ and $\lim_{\xi\to\infty}(U(\xi), V(\xi)) = \mathbf{X}_R$. Here $\mathbf{X}_L$ denotes the activity during left eye dominance while $\mathbf{X}_R$ denotes activity during right eye dominance. We define left eye and right eye dominant states in terms of fixed points of the dynamical system in Eqs. (2.1) and (2.2). Finally, we must have that $U(\xi)$ and $V(\xi)$ cross the threshold κ at some point. Since Eqs. (2.1) and (2.2) are invariant to translations, we may allow $U(\xi)$ to cross threshold at any arbitrary point. However, the distance between the threshold crossing values cannot be arbitrary. Therefore we can let $U(0) = V(\xi_0) = \kappa$.

3.1. Fixed points

We first search for homogeneous fixed point solutions (U^*, V^*, Q_u^*, Q_v^*). Using the Heaviside firing function and plugging these into Eqs. (2.1) and (2.2) we obtain

$$U^* = I_u + Q_u^* A_e H(U-\kappa) - Q_v^* A_i H(V-\kappa), \tag{3.1a}$$

$$V^* = I_v + Q_v^* A_e H(V-\kappa) - Q_u^* A_i H(U-\kappa), \tag{3.1b}$$

$$Q_u^* = \frac{1}{1+\beta H(U-\kappa)}, \tag{3.1c}$$

$$Q_v^* = \frac{1}{1+\beta H(V-\kappa)}, \tag{3.1d}$$

where

$$A_e = \int_{-\infty}^{\infty} w_{e\pm}(x)dx, \tag{3.2a}$$

$$A_i = \int_{-\infty}^{\infty} w_i(x)dx. \tag{3.2b}$$

There are four possible homogeneous fixed points corresponding to an off-state, a fusion state and two winner-take-all (WTA) states. The fusion state is given by

$$(U^*, V^*) = \left(\frac{A_e - A_i}{1+\beta} + I_u, \frac{A_e - A_i}{1+\beta} + I_v\right), \tag{3.3a}$$

$$(Q_u^*, Q_v^*) = \left(\frac{1}{1+\beta}, \frac{1}{1+\beta}\right), \tag{3.3b}$$

and occurs when $I_u, I_v > \kappa - (A_e - A_i)/(1+\beta)$. The left eye dominant WTA state is given by

$$(U^*, V^*) = \left(\frac{A_e}{1+\beta} + I_u, I_v - \frac{A_i}{1+\beta}\right), \tag{3.4a}$$

$$(Q_u^*, Q_v^*) = \left(\frac{1}{1+\beta}, 1\right), \tag{3.4b}$$

which occurs when $I_u > \kappa - A_e/(1+\beta)$ and $I_v < \kappa + A_i/(1+\beta)$. On the other hand, the right eye dominant WTA state is

$$(U^*, V^*) = \left(I_u - \frac{A_i}{1+\beta}, \frac{A_e}{1+\beta} + I_v\right), \tag{3.5a}$$

$$(Q_u^*, Q_v^*) = \left(1, \frac{1}{1+\beta}\right), \tag{3.5b}$$

which occurs when $I_v > \kappa - A_e/(1+\beta)$ and $I_u < \kappa + A_i/(1+\beta)$. Finally the off state is simply $(U, V) = (I_u, I_v)$ and $(Q_u, Q_v) = (1, 1)$ which occurs when $I_u, I_v < \kappa - (A_e - A_i)/(1+\beta)$. It has been shown elsewhere that all the fixed points of the space-clamped network are linearly stable so that a limit cycle cannot occur via a Hopf bifurcation, rather oscillations occur via an escape mechanism [32]. Moreover, the oscillatory rivalry state coexists with the fusion state when the inputs I_u and I_v are greater than those values in which a WTA state exists ($I_u, I_v > \kappa + A_i/(1+\beta)$). Since we would like the traveling wave solutions to coexist with the space clamped rivalry state, we will use this inequality in the analysis for existence of traveling waves.

3.2. Non-depressing synapses ($\beta = 0$)

Consider the simpler case of no synaptic depression, $\beta = 0$, so that $q_u = q_v \equiv 1$, $\mathbf{X}_L = (A_e + I_u, I_v - A_i)$ and $\mathbf{X}_R = (I_u - A_i, A_e + I_v)$. Bressloff and Webber [9] have previously established that, in the case of symmetric weights, traveling waves cannot exist without synaptic depression. We first check that the same result holds for asymmetric weights. Using the Heaviside firing rate function and applying integrating factors to Eqs. (2.1) and (2.2), we find that

$$U(\xi) = \frac{1}{c}\int_{\xi}^{\infty} e^{(\xi-\xi')/c}\left[W_{e+}(\xi') - W_i(\xi_0 - \xi')\right]d\xi' + I_u, \tag{3.6a}$$

$$V(\xi) = \frac{1}{c}\int_{\xi}^{\infty} e^{(\xi-\xi')/c}\left[W_{e+}(\xi_0 - \xi') - W_i(\xi')\right]d\xi' + I_v, \tag{3.6b}$$

where

$$W_p(x) = \int_x^{\infty} w_p(y)dy \tag{3.7}$$

for $p = e+, e-, i$. Imposing the threshold crossing conditions, we obtain a pair of implicit equations for the wave speed c and ξ_0:

$$\kappa = W_{e+}(0) - W_i(\xi_0) - \int_0^{\infty} e^{-\xi/c}\left[w_{e+}(\xi) - w_i(\xi - \xi_0)\right]d\xi + I_u, \tag{3.8a}$$

$$\kappa = W_{e+}(0) - W_i(\xi_0) + \int_0^\infty e^{-\xi/c}\left[w_{e+}(\xi) + w_i(\xi+\xi_0)\right]d\xi + I_v. \tag{3.8b}$$

Subtracting (3.8a) from (3.8b) gives

$$0 = \int_0^\infty e^{-\xi/c}\left[w_{e+}(\xi) + w_{e-}(\xi) + w_i(\xi-\xi_0) + w_i(\xi+\xi_0)\right]d\xi + I_v - I_u \equiv F(c, x_0, \xi_0). \tag{3.9}$$

Note that for $I_u = I_v$

$$\lim_{c\to 0} F(c, x_0, \xi_0) = 0 \tag{3.10}$$

and $F(c, x_0, \xi_0)$ is monotonically increasing, so that only speed at which the equation is satisfied is $c = 0$. Therefore there are no traveling wave solutions in the absence of synaptic depression. The existence of a non-zero wave speed arises when $I_u \neq I_v$, however binocular rivalry is known to occur even when $I_u = I_v$. Therefore we must consider additional mechanisms that induce traveling waves, such as the presence of synaptic depression.

3.3. Slow synaptic depression ($\beta > 0$, $\tau_s \gg 1$)

We now include synaptic depression by looking for traveling wave solutions in both the activity variables (as before) and in the depression variables, with the latter given by $q_u(x,t) = Q_u(\xi)$ and $q_v(x,t) = Q_v(\xi)$ such that $\lim_{\xi\to-\infty}(Q_u(\xi), Q_v(\xi)) = ((1+\beta)^{-1}, 1)$ and $\lim_{\xi\to\infty}(Q_u(\xi), Q_v(\xi)) = (1, (1+\beta)^{-1})$. Additionally we take the left and right activity states to be $\mathbf{X}_L = (A_e/(1+\beta) + I_u, I_v - A_i/(1+\beta))$ and $\mathbf{X}_R = (I_u - A_i/(1+\beta), A_e/(1+\beta) + I_v)$. Substituting the full traveling wave solution into Eqs. (2.1) and (2.2) yields

$$Q_u(\xi) = \begin{cases} \dfrac{1}{1+\beta}\left[1+\beta e^{\xi(1+\beta)/c\tau_s}\right], & \text{for } \xi \le 0 \\ 1, & \text{for } \xi \ge 0 \end{cases} \tag{3.11a}$$

$$Q_v(\xi) = \begin{cases} 1 - \dfrac{\beta}{1+\beta} e^{(\xi-\xi_0)/c\tau_s}, & \text{for } \xi \le \xi_0 \\ \dfrac{1}{1+\beta}, & \text{for } \xi \ge \xi_0 \end{cases} \tag{3.11b}$$

and

$$U(\xi) = \frac{1}{c}\int_\xi^\infty e^{\frac{\xi-\xi'}{c}}\left[\overline{W}_{e,u}(\xi') - \overline{W}_{i,v}(\xi_0-\xi')\right]d\xi' + I_u, \tag{3.12a}$$

$$V(\xi) = \frac{1}{c}\int_\xi^\infty e^{\frac{\xi-\xi'}{c}}\left[\overline{W}_{e,v}(\xi_0-\xi') - \overline{W}_{i,u}(\xi')\right]d\xi' + I_v, \tag{3.12b}$$

where

$$\overline{W}_{e,u}(x) = \int_x^\infty w_{e+}(y)Q_u(x-y)dy, \tag{3.13a}$$

$$\overline{W}_{e,v}(x) = \int_x^\infty w_{e+}(y)Q_v(y-x+\xi_0)dy = \frac{1}{1+\beta}\int_x^\infty w_{e+}(y)dy = \frac{1}{1+\beta}W_e(x), \tag{3.13b}$$

$$\overline{W}_{i,u}(x) = \int_x^\infty w_i(y)Q_u(x-y)dy, \tag{3.13c}$$

$$\overline{W}_{i,v}(x) = \int_x^\infty w_i(y)Q_v(y-x+\xi_0)dy = \frac{1}{1+\beta}\int_x^\infty w_i(y)dy = \frac{1}{1+\beta}W_i(x), \tag{3.13d}$$

where the second and fourth equalities come from the fact that, when integrating in the region $y > x$, we have $Q_v(y-x+\xi_0) = 1$. Again, imposing threshold conditions we have the implicit equation

$$F(c, x_0, \xi_0) \equiv \frac{1}{c}\int_0^\infty e^{-\frac{\xi'}{c}}\left[\overline{W}_{e,u}(\xi') - \overline{W}_{e,v}(-\xi') + \overline{W}_{i,u}(\xi'+\xi_0) - \overline{W}_{i,v}(\xi_0-\xi')\right] + I_u - I_v = 0. \tag{3.14}$$

It can be shown that both $F(c, x_0, \xi_0)$ is an increasing function of c and

$$\lim_{c\to 0} F(c, x_0, \xi_0) = 0 \tag{3.15}$$

for $I_u = I_v$, so that only $c = 0$ satisfies the implicit equation and no traveling wave solutions exist. This result is not surprising considering that all of the fixed points are stable so that no heteroclinic orbits exist between the states.

Nevertheless, as previously shown by Bressloff and Webber [9] for symmetric weights, a traveling wave solution does exist in the case of fixed depression variables with $Q_u \neq Q_v$. This adiabatic approximation can be used when the network is in a binocular rivalry state provided that (a) the duration of the wave propagation is short compared to the natural switching period and (b) the induction of the wave does not occur close to the point at which spontaneous switching occurs [9]. (One possible alternative to this approach would be to perturb the differential equations for the depression variables.) With the adiabatic approximation in mind, consider the modified system of neural field equations given by

$$\frac{\partial u(x,t)}{\partial t} = -u(x,t) + I_u + Q_u\int_{-\infty}^\infty w_{e+}(x-x')f(u(x',t))dx' - Q_v\int_{-\infty}^\infty w_i(x-x')f(v(x',t))dx' \tag{3.16a}$$

$$\frac{\partial v(x,t)}{\partial t} = -v(x,t) + I_v + Q_v\int_{-\infty}^\infty w_{e-}(x-x')f(v(x',t))dx' - Q_u\int_{-\infty}^\infty w_i(x-x')f(u(x',t))dx'. \tag{3.16b}$$

Note that since Q_u and Q_v are now arbitrary, the asymptotic left and right eye activity states are redefined as $\mathbf{X}_L = (I_u + Q_uA_e, I_v - Q_uA_i)$ and $\mathbf{X}_R = (I_u - Q_vA_i, I_v + Q_vA_e)$. In order for the waves to cross the threshold κ, we require that both $\kappa - Q_uA_e < I_u < \kappa + Q_vA_i$ and $\kappa - Q_vA_e < I_v < \kappa + Q_uA_i$. Under the adiabatic approximation, the solutions have the same form as (3.12a) and (3.12b), after replacing all the synaptic depression solutions by a constant. The threshold conditions become

$$\kappa = I_u + Q_uW_{e+}(0) - Q_vW_i(\xi_0) - \int_0^\infty e^{-\xi'/c_+}\left[Q_uw_{e+}(\xi') + Q_vw_i(\xi'-\xi_0)\right]d\xi' \equiv F_1^+(c_+, x_0, \xi_0) \tag{3.17a}$$

$$\kappa = I_v + Q_vW_{e+}(0) - Q_uW_i(\xi_0) + \int_0^\infty e^{-\xi'/c_+}\left[Q_uw_i(\xi+\xi_0) + Q_vw_{e-}(\xi)\right]d\xi' \equiv F_2^+(c_+, x_0, \xi_0) \tag{3.17b}$$

and Eq. (3.14) becomes

$$F^+(c_+, x_0, \xi_0) \equiv \Delta I + (Q_u - Q_v)(W_{e+}(0) + W_i(\xi_0)) - \int_0^\infty e^{-\xi'/c_+}[Q_u(w_{e+}(\xi') + w_i(\xi'+\xi_0)) + Q_v(w_{e-}(\xi') + w_i(\xi-\xi_0))]d\xi' = 0 \tag{3.18}$$

where $\Delta I = I_u - I_v$. Note that we have introduced the index $+$ on F^+ and c_+ to indicate that we are looking for positive wave speeds with respect to the sign of the shift x_0, which corresponds to the

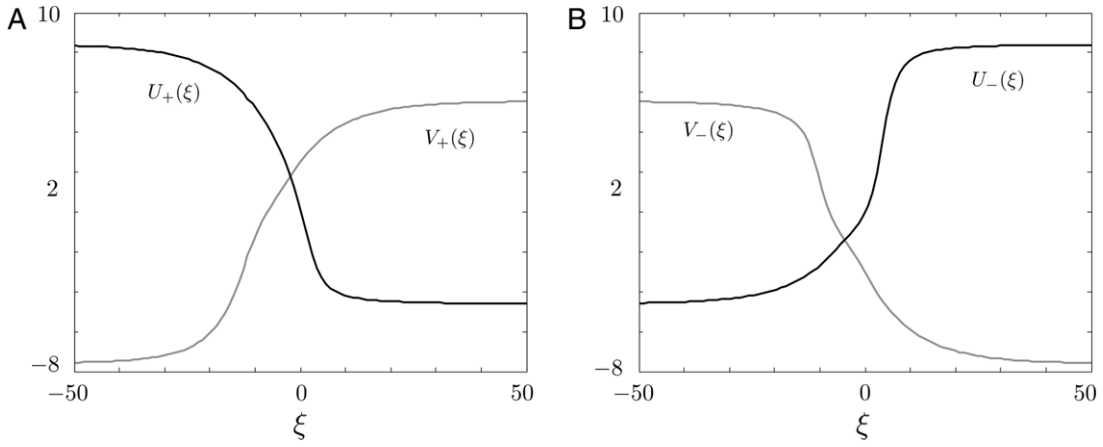

Fig. 4. Plot of profiles in the co-moving frame $\xi = x - ct$ for wave fronts traveling in the positive (left) and negative (right) directions. Exponential weight functions were used with the following parameters: $a_e = 4$, $\sigma_e = 0.42$, $x_0 = 2$, $a_i = 1$, $\sigma_i = 0.1$. Other parameters used: $\kappa = 0.05$, $Q_u = 0.42$, $Q_v = 0.25$, $I_u = 0.4$, $I_v = 0.8$.

case in which rivalry waves move in the same direction as the carrier stimulus, see Fig. 3; we will consider negative wave speeds later. If $Q_u > Q_v > 0$ and $I_u \leq I_v$ with $|\Delta I|$ sufficiently small, then

$$\lim_{c_+\to 0} F^+(c_+, x_0, \xi_0) = (Q_u - Q_v)(W_{e+}(0) + W_i(\xi_0)) + \Delta I > 0, \tag{3.19a}$$

$$\lim_{c_+\to \infty} F^+(c_+, x_0, \xi_0) = -Q_v(W_{e+}(0) + W_{e-}(0) + W_i(\xi_0) + W_i(-\xi_0)) + \Delta I < 0. \tag{3.19b}$$

Note that the second inequality always holds, whereas the first inequality is satisfied provided that $|\Delta I|$ is small enough. Since $F_+(c_+, x_0, \xi_0)$ is continuous, the intermediate value theorem guarantees existence of a solution $c_+(x_0, \xi_0) > 0$ such that $F_+(c_+(x_0, \xi_0), x_0, \xi_0) = 0$. Given the solution $c_+ = c_+(x_0, \xi_0)$, existence of a traveling wave solution is guaranteed by the implicit function theorem and is determined by the single threshold condition Eq. (3.17a). It can be shown that a wave exists provided that

$$Q_v(W_i(\xi_0) + W_i(-\xi_0)) + \kappa > I_u > \kappa + Q_v W_i(\xi_0) - Q_u W_{e+}(0). \tag{3.20}$$

Note that $W_i(\xi_0) + W_i(-\xi_0) = A_i$, so that the upper limit follows from the inequality imposed on I_u in order to ensure the wave crosses threshold. The lower limit holds for appropriate choices of parameters such that

$$A_e > 2(A_i + \kappa(1 + \beta)). \tag{3.21}$$

This can be seen by noting that $W_{e+}(0) > \frac{1}{2}A_e$ for all $x_0 > 0$, $W_i(\xi_0) < A_i$ for all ξ_0 and $Q_u > Q_v > 1/(1+\beta)$, so that

$$Q_u W_{e+}(0) - Q_v W_i(\xi_0) - \kappa > Q_v\left(\frac{1}{2}A_e - A_i\right) - \kappa > 0. \tag{3.22}$$

Thus we have that $I_u > 0 > \kappa + Q_v W_i(\xi_0) - Q_u W_{e+}(0)$. This inequality is reasonable to impose since it essentially states that the total strength of inhibition cannot be too large. An example wave profile is shown in Fig. 4(a).

We now consider existence of a traveling wave propagating in the negative direction relative to the shift x_0. In doing so we now require that $\lim_{\xi\to-\infty}(U_-(\xi), V_-(\xi)) = \mathbf{X}_R$ and $\lim_{\xi\to\infty}(U_-(\xi), V_-(\xi)) = \mathbf{X}_L$ as well as the threshold conditions, $U_-(0) = \kappa$ and $V_-(\xi_{0-}) = \kappa$. Proceeding along similar lines to the case of positive speed solutions, we find that

$$U_-(\xi) = -\frac{1}{c_-}\int_{-\xi}^{\infty} e^{(\xi+\xi')/c_-}\left[Q_u W_{e-}(\xi') - Q_u W_i(-\xi' - \xi_{0-})\right]d\xi' + I_u, \tag{3.23a}$$

$$V_-(\xi) = -\frac{1}{c_-}\int_{-\xi}^{\infty} e^{(\xi+\xi')/c_-}\left[Q_v W_{e-}(-\xi' - \xi_{0-}) - Q_u W_i(\xi')\right]d\xi' + I_v. \tag{3.23b}$$

Imposing the threshold conditions gives

$$\kappa = I_u + Q_u W_{e-}(0) - Q_v W_i(-\xi_{0-}) - \int_0^{\infty} e^{-\frac{\xi'}{|c_-|}}\left[Q_u w_{e-}(\xi') + Q_v w_i(\xi + \xi_{0-})\right]d\xi' \equiv F_1^-(c_-, x_0, \xi_{0-}), \tag{3.24a}$$

$$\kappa = I_v - Q_u W_i(-\xi_{0-}) + Q_v W_{e-}(0) + \int_0^{\infty} e^{-\frac{\xi'}{|c_-|}}\left[Q_u w_i(\xi' - \xi_{0-}) + Q_v w_{e+}(\xi')\right]d\xi' \equiv F_2^-(c_-, x_0, \xi_{0-}). \tag{3.24b}$$

Subtracting Eqs. (3.24a) and (3.24b) yields the implicit equation

$$F^-(c_-, x_0, \xi_0) \equiv \Delta I + (Q_u - Q_v)(W_{e-}(0) + W_i(-\xi_{0-})) - \int_0^{\infty} e^{-\frac{\xi}{|c_-|}}[Q_u(w_{e-}(\xi) + w_i(\xi_{0-} - \xi)) + Q_v(w_{e+}(\xi) + w_i(\xi_{0-} + \xi))]d\xi = 0. \tag{3.25}$$

Similar to positive wave speeds, we find that for $Q_u > Q_v$

$$\lim_{|c_-|\to 0} F^-(c_-, x_0, \xi_{0-}) = (Q_u - Q_v)(W_{e-}(0) + W_i(-\xi_{0-})) + \Delta I, \tag{3.26a}$$

$$\lim_{|c_-|\to \infty} F^-(c_-, x_0, \xi_{0-}) = -Q_v(W_{e+}(0) + W_{e-}(0) + W_i(\xi_{0-}) + W_i(-\xi_{0-})) < 0. \tag{3.26b}$$

Again, there exists a solution $c_- = c_-(x_0, \xi_{0-})$ such that $F^-(c_-, x_0, \xi_{0-}) = 0$ provided that $\lim_{|c_-|\to 0} F^- > 0$. However, in contrast to the positive wave speed case, this latter inequality does not necessarily hold for all $x_0 > 0$. In order to show this, note that $W_{e-}(0) \to 0$ as $x_0 \to \infty$ and, as we show in Section 5.1, ξ_{0-} is a monotonically decreasing function of x_0 so that $W_i(-\xi_{0-}(x_0)) \to \omega_0$ for some constant ω_0 as $x_0 \to \infty$. If $\omega_0 + \Delta I < 0$ then there exists an x_0^* such that

$$\lim_{|c-|\to 0} F^-(c_-, x_0^*, \xi_{0-}(x_0^*)) = 0, \tag{3.27}$$

in which case the only solution is $c_- = 0$. Thus existence of a negative wave speed disappears at $c_-(x_0^*) = 0$, so that no traveling waves exist for $x_0 > x_0^*$. Given the solution $c_- = c_-(x_0, \xi_{0-})$ for $x_0 \in [0, x_0^*)$, existence of a traveling wave solution is determined

by the single threshold condition given by Eq. (3.24a). It is then easy to show that a wave exists provided

$$Q_v(W_i(-\xi_{0-}) + W_i(\xi_{0-})) + \kappa > I_u > Q_v W_i(-\xi_{0-}) - Q_u W_{e-}(0) + \kappa, \tag{3.28}$$

which is consistent with the constraints already imposed on I_u. An example of a negative speed wave profile is shown in Fig. 4(b).

4. Stability

To determine linear stability of traveling wave solutions $U(\xi)$ and $V(\xi)$, we perturb solutions by the functions $\psi(\xi, t)$ and $\varphi(\xi, t)$ so that

$$U(\xi, t) = U(\xi) + \psi(\xi, t), \tag{4.1a}$$

$$V(\xi, t) = V(\xi) + \varphi(\xi, t). \tag{4.1b}$$

Substituting these into Eqs. (2.1) and (2.2) and linearizing about $U(\xi)$ and $V(\xi)$ yield

$$\frac{\partial \Psi(\xi, t)}{\partial t} = \mathcal{L}\Psi(\xi, t) \equiv \left(c\frac{\partial}{\partial \xi} - I\right)\Psi(\xi, t) + \int_{-\infty}^{\infty} A(\xi, \xi')\Psi(\xi, t)d\xi', \tag{4.2}$$

where $\Psi(\xi, t) = (\psi(\xi, t), \varphi(\xi, t))^T$ and

$$A(\xi, \xi') = \begin{pmatrix} Q_u w_{e+}(\xi - \xi')f'(U(\xi')) & -Q_v w_i(\xi - \xi')f'(V(\xi')) \\ -Q_u w_i(\xi - \xi')f'(U(\xi')) & Q_v w_{e-}(\xi - \xi')f'(V(\xi')) \end{pmatrix}. \tag{4.3}$$

Looking for solutions of the form $\Psi(\xi, t) = \Psi(\xi)e^{\lambda t}$ we have the spectral problem $\lambda\Psi(\xi) = \mathcal{L}\Psi(\xi)$. Here we take the linear operator $\mathcal{L} : W^{1,1}(\mathbb{R}, \mathbb{R}^2) \to W^{1,1}(\mathbb{R}, \mathbb{R}^2)$ to act on vector valued functions whose elements belong to the Sobolev space $W^{1,1}(\mathbb{R})$, which is a Banach space. That is if $\Psi \in W^{1,1}(\mathbb{R})$ then $\Psi, \Psi' \in L^1(\mathbb{R})$. The motivation for this choice of a function space is that we want to consider localized perturbations to traveling wave solutions. Therefore we consider functions that decay to zero fast enough in space. The wave will be linearly stable if all non-zero $\lambda \in \sigma(\mathcal{L})$, the spectrum of $\mathcal{L}$, have negative real part and $\lambda = 0$ is a simple eigenvalue [9]. Recall that the complex plane can be divided into two sets: the spectrum $\sigma(\mathcal{L})$ and the resolvent set $\rho(\mathcal{L})$. Furthermore, the spectrum itself can be decomposed into the sum of the point spectrum $\sigma_p(\mathcal{L})$ and the essential spectrum $\sigma_{ess}(\mathcal{L})$. We say that $\lambda \in \sigma_p(\mathcal{L})$ if λ is an eigenvalue of $\mathcal{L}$ (the resolvent operator $R_\lambda = (\mathcal{L} - \lambda I)^{-1}$ does not exist) while $\lambda \in \sigma_{ess}(\mathcal{L})$ if R_λ exists, but is unbounded and not defined on a dense subset of $W^{1,1}(\mathbb{R}, \mathbb{R}^2)$. We proceed by first finding eigenvalues of the operator $\mathcal{L}$ and points in the resolvent set $\rho(\mathcal{L})$ ($\lambda \in \mathbb{C}$ such that R_λ exists, is bounded and is defined on a dense subset of $W^{1,1}(\mathbb{R}, \mathbb{R}^2)$) as these are the most straightforward values to find.

Note that for a Heaviside firing rate function we have that $f'(U(\xi)) = \frac{\delta(\xi)}{|U'(0)|}$ and $f'(V(\xi)) = \frac{\delta(\xi - \xi_0)}{|V'(\xi_0)|}$ so that we can write Eq. (4.2) as

$$\left(\frac{\partial}{\partial \xi} - \frac{\lambda + 1}{c}\right)\Psi(\xi) + B(\xi)\overline{\Psi} = 0, \tag{4.4}$$

where

$$B(\xi) = \begin{pmatrix} \frac{Q_u w_{e+}(\xi)}{c|U'(0)|} & -\frac{Q_v w_i(\xi - \xi_0)}{c|V'(\xi_0)|} \\ -\frac{Q_u w_i(\xi)}{c|U'(0)|} & \frac{Q_v w_{e-}(\xi - \xi_0)}{c|V'(\xi_0)|} \end{pmatrix}, \tag{4.5}$$

and $\overline{\Psi} = (\psi(0), \varphi(\xi_0))^T$. Multiplying by $e^{-(\lambda+1)\xi/c}$ and integrating yield

$$\Psi(\xi) = \int_{\xi}^{\infty} e^{\frac{\lambda+1}{c}(\xi - \xi')}B(\xi')\overline{\Psi}d\xi' \tag{4.6}$$

and imposing self-consistency we have the equation given in Box I. This has a non-trivial solution provided that λ is a zero of the Evans function [9,36–38]

$$\mathcal{E}(\lambda) = \det(M(\lambda)). \tag{4.8}$$

That is, the complex number λ is an eigenvalue of the linear system if and only if $\mathcal{E}(\lambda) = 0$. The existence of a zero eigenvalue, with corresponding eigenfunction $\Psi(\xi) = (U'(\xi), V'(\xi))^T$, reflects the translation invariance of the traveling wave solutions. Attempting to solve for other eigenvalues, we find that $\lambda = 0$ is the only solution. That is, the only $\lambda \in \mathbb{C}$ in the point spectrum of the linear operator $\mathcal{L}$ is $\lambda = 0$.

To compute $\lambda \in \rho(\mathcal{L})$, the resolvent set, we consider solving the problem $\mathcal{R}_\lambda h = \Psi$. This is equivalent to solving the equation

$$\left(\frac{\partial}{\partial \xi} - \frac{\lambda + 1}{c}\right)\Psi(\xi) + B(\xi)\overline{\Psi} = h(\xi) \tag{4.9}$$

for $\Psi(\xi)$. By imposing self consistency, we find that we can uniquely solve for $\overline{\Psi}$ as

$$\overline{\Psi} = M(\lambda)^{-1}\begin{pmatrix} \int_0^{\infty} e^{-\frac{\lambda+1}{c}\xi'}h_1(\xi')d\xi' \\ \int_{\xi_0}^{\infty} e^{-\frac{\lambda+1}{c}(\xi' - \xi_0)}h_2(\xi')d\xi' \end{pmatrix}. \tag{4.10}$$

We know that $M(\lambda)$ is invertible since we are considering $\lambda \notin \sigma_p(\mathcal{L})$, so that $\det(M(\lambda)) = \mathcal{E}(\lambda) \neq 0$. Therefore we can solve for $\Psi(\xi)$ in terms of $h(\xi)$ as

$$\Psi(\xi) = \mathcal{R}_\lambda h(\xi) = \int_{\xi}^{\infty} e^{\frac{\lambda+1}{c}(\xi - \xi')}\left[B(\xi')\overline{\Psi} - h(\xi')\right]d\xi', \tag{4.11}$$

which is well-defined for all $h \in W^{1,1}(\mathbb{R}, \mathbb{R}^2)$ when $\mathrm{Re}(\lambda) > -1$ and $\lambda \neq 0$. Therefore the resolvent set is $\rho(\mathcal{L}) = \{\lambda \in \mathbb{C} | \mathrm{Re}(\lambda) > -1, \lambda \neq 0\}$. Thus we have that the spectrum of the linear operator is given by $\sigma(\mathcal{L}) = \{0\} \cup \{\lambda \in \mathbb{C} | \mathrm{Re}(\lambda) \leq -1\}$, since $\mathbb{C} = \rho(\mathcal{L}) \cup \sigma(\mathcal{L})$. Since the real part of all of the non-zero elements in the spectrum is strictly negative and zero is a simple eigenvalue, we have that traveling wave solutions are stable.

5. Stimulus motion determines wave speed

We now use our analysis to determine how wave speed varies with the shift x_0 in the recurrent weights, and show that the speed of propagation is greater for the wave traveling in the direction of the low contrast stimulus, as previously observed in the experimental and computational study of Knapen et al. [13]. We also show that, in contrast to asymmetric spatial decay rates [13], an asymmetric shift in the cross-inhibition cannot account for the differences in wave speed.

5.1. Asymmetry in excitation

Recall the implicit equations $F_+(c_+, x_0, \xi_{0+}) = 0$ and $F_-(c_-, x_0, \xi_{0-}) = 0$, see (3.18) and (3.25), which determine the positive and negative wave speeds respectively. Note that if $x_0 = 0$ then $w_{e-}(x) = w_{e+}(x)$ so that $F_+(c_+, x_0, \xi_{0+}) = F_-(c_-, x_0, \xi_{0-})$ when $|c_-| = c_+$ and $\xi_{0-} = -\xi_{0+}$. This shows that when stationary stimuli are used, the traveling waves propagate at the same speed in both directions and the traveling wave solutions are reflections of

$$M(\lambda)\overline{\Psi} = \begin{pmatrix} \frac{Q_u}{c|U'(0)|}\int_0^\infty e^{-\frac{\lambda+1}{c}\xi} w_{e+}(\xi)d\xi - 1 & -\frac{Q_v}{c|V'(\xi_0)|}\int_0^\infty e^{-\frac{\lambda+1}{c}\xi} w_i(\xi-\xi_0)d\xi \\ -\frac{Q_u}{c|U'(0)|}\int_0^\infty e^{-\frac{\lambda+1}{c}\xi} w_i(\xi+\xi_0)d\xi & \frac{Q_v}{c|V'(\xi_0)|}\int_0^\infty e^{-\frac{\lambda+1}{c}\xi} w_{e-}(\xi) - 1 \end{pmatrix} \begin{pmatrix} \psi(0) \\ \varphi(\xi_0) \end{pmatrix} = 0. \tag{4.7}$$

Box I.

one another. For $x_0 > 0$ we can determine the relationship between c_- and c_+ by implicitly differentiating Eqs. (3.17a), (3.17b), (3.24a) and (3.24b). Noting that

$$\begin{aligned} \frac{dF_1^+(c_+(x_0,\xi_0),x_0,\xi_0)}{dx_0} &= \frac{dF_2^+(c_+(x_0,\xi_0),x_0,\xi_0)}{dx_0} \\ &= \frac{dF_1^-(c_-(x_0,\xi_0),x_0,\xi_0)}{dx_0} \\ &= \frac{dF_2^-(c_-(x_0,\xi_0),x_0,\xi_0)}{dx_0} = 0, \end{aligned}$$

we have

$$\begin{pmatrix} \frac{dc_+}{dx_0} \\ \frac{d\xi_0}{dx_0} \end{pmatrix} = -\begin{pmatrix} \frac{\partial F_1^+}{\partial c+} & \frac{\partial F_1^+}{\partial \xi_0} \\ \frac{\partial F_2^+}{\partial c+} & \frac{\partial F_2^+}{\partial \xi_0} \end{pmatrix}^{-1} \begin{pmatrix} \frac{\partial F_1^+}{\partial x_0} \\ \frac{\partial F_2^+}{\partial x_0} \end{pmatrix} \tag{5.1}$$

and a similar expression for $|c_-|$ and ξ_{0-}. Solving for dc_+/dx_0 and $d\xi_0/dx_0$ gives

$$\frac{1}{c_+}\frac{dc_+}{dx_0} = \frac{Q_u^2 G[w_{e+}(\xi)]G[w_{i-}(\xi)] - Q_v^2 G[w_{e-}(\xi)]G[w_{i+}(\xi)]}{G[w_{i-}(\xi)]\Gamma_1(c_+,\xi_0,Q_u,Q_v) + G[w_{i+}(\xi)]\Gamma_2(c_+,\xi_0,Q_u,Q_v)}, \tag{5.2}$$

and

$$\frac{d\xi_0}{dx_0} = -\frac{1}{Q_u Q_v}\frac{Q_u^2 G[w_{e+}(\xi)]\Gamma_2(c_+,\xi_0,Q_u,Q_v) + Q_v^2 G[w_{e-}(\xi)]\Gamma_1(c_+,\xi_0,Q_u,Q_v)}{G[w_{i-}(\xi)]\Gamma_1(c_+,\xi_0,Q_u,Q_v) + G[w_{i+}(\xi)]\Gamma_2(c_+,\xi_0,Q_u,Q_v)}, \tag{5.3}$$

where $w_{i\pm}(\xi) = w_i(\xi \mp \xi_0)$,

$$\begin{aligned} G[f(\xi)] &= \int_0^\infty e^{-\xi/c_+} f(\xi)d\xi, \\ H[f(\xi)] &= \int_0^\infty \xi e^{-\xi/c_+} f(\xi)d\xi, \end{aligned} \tag{5.4}$$

and

$$\begin{aligned} \Gamma_1(c_+,\xi_0,Q_u,Q_v) &= Q_u^2 H[w_{e+}(\xi)] + Q_u Q_v H[w_{i+}(\xi)], \\ \Gamma_2(c_+,\xi_0,Q_u,Q_v) &= Q_v^2 H[w_{e-}(\xi)] + Q_u Q_v H[w_{i-}(\xi)]. \end{aligned} \tag{5.5}$$

The functionals G and H are strictly positive when $f(\xi) > 0$ for all $\xi > 0$. It follows that ξ_0 is a monotonically decreasing function of x_0, since both of the terms in the numerator and denominator of Eq. (5.3) are positive for all $x_0 > 0$. To determine the sign of dc_+/dx_0 we need only consider the term in the numerator of Eq. (5.2), since the term in the denominator is always positive. Additionally, it is sufficient to show that $A(x_0) \equiv Q_u^2 G[w_{i-}(\xi)] - Q_v^2 G[w_{i-}(\xi)] > 0$ for all $\xi_0 = \xi_0(x_0)$ as $w_{e+}(\xi) > w_{e-}(\xi)$ for all $\xi > 0$. The inequality $A(x_0) > 0$ certainly holds if $\xi_0(0) < 0$ since $w_i(\xi+\xi_0) > w_i(\xi-\xi_0)$ for all $\xi_0 < 0$ and ξ_0 is decreasing so that $\xi_0(x_0) < \xi_0(0) < 0$ for all $x_0 > 0$. The proof is less obvious if $\xi_0(0) > 0$. Nevertheless, if $\xi_0(0)$ is small enough then one can find values of Q_u and Q_v such that

$$Q_u^2 w_i(2\xi_0(0)) > Q_v^2 w_i(\xi(0)) \tag{5.6}$$

and, since ξ_0 is decreasing, Eq. (5.6) holds for all $\xi_0(x_0)$. Under these conditions, $A(x_0) > 0$ for all $x_0 > 0$ and c_+ is a monotonically increasing function of x_0.

Similarly, solving for dc_-/dx_0 and $d\xi_{0-}/dx_0$ gives

$$\frac{1}{|c_-|}\frac{d|c_-|}{dx_0} = \frac{-Q_u^2 G[w_{e-}(\xi)]G[w_{i+}(\xi)] + Q_v^2 G[w_{e+}(\xi)]G[w_{i-}(\xi)]}{G[w_{i+}(\xi)]\Gamma_1(c_-,\xi_{0-},Q_u,Q_v) + G[w_{i-}(\xi)]\Gamma_2(c_-,\xi_{0-},Q_u,Q_v)}, \tag{5.7}$$

and

$$\frac{d\xi_{0-}}{dx_0} = -\frac{1}{Q_u Q_v} \times \frac{Q_u^2 G[w_{e-}(\xi)]\Gamma_2(c_-,\xi_{0-},Q_u,Q_v) + Q_v^2 G[w_{e+}(\xi)]\Gamma_1(c_-,\xi_{0-},Q_u,Q_v)}{G[w_{i+}(\xi)]\Gamma_1(c_-,\xi_{0-},Q_u,Q_v) + G[w_{i-}(\xi)]\Gamma_2(c_-,\xi_{0-},Q_u,Q_v)}, \tag{5.8}$$

where now

$$\begin{aligned} G[f(\xi)] &= \int_0^\infty e^{-\xi/|c_-|} f(\xi)d\xi, \\ H[f(\xi)] &= \int_0^\infty \xi e^{-\xi/|c_-|} f(\xi)d\xi. \end{aligned} \tag{5.9}$$

and

$$\begin{aligned} \Gamma_1(c_-,\xi_{0-},Q_u,Q_v) &= Q_u^2 H[w_{e-}(\xi)] + Q_u Q_v H[w_{i-}(\xi)], \\ \Gamma_2(c_+,\xi_0,Q_u,Q_v) &= Q_v^2 H[w_{e+}(\xi)] + Q_u Q_v H[w_{i+}(\xi)]. \end{aligned} \tag{5.10}$$

Again, we see that ξ_{0-} is a monotonically decreasing function of x_0 so that the analysis for the existence of negative wave speeds in Section 3.3 holds. When $x_0 = 0$, we know that $w_{e-}(x) = w_{e+}(x)$, $\xi_{0-} = -\xi_0$ and $c_- = -c_+$ so that

$$\left.\frac{d|c_-|}{dx_0}\right|_{x_0=0} = -\left.\frac{dc_+}{dx_0}\right|_{x_0=0}. \tag{5.11}$$

Hence, if c_+ is increasing at $x_0 = 0$ then $|c_-|$ is decreasing at $x_0 = 0$. Thus in a neighborhood of $x_0 = 0$, $c_+ > |c_-|$. Suppose that there is a point at which $|c_-| > c_+$ for $x_0 \neq 0$. It follows that there must have been a value $x_0^* \neq 0$ at which $|c_-| = c_+$. Subtracting Eq. (3.25) from Eq. (3.18) with $|c_-| = c_+$ requires that $F^+(c_+,x_0,\xi_0) - F^-(c_+,x_0,\xi_{0-}) = 0$. However,

$$\begin{aligned} \lim_{c_+\to 0}[F^+ - F^-] &= (Q_u - Q_v)(W_{e+}(0) \\ &\quad - W_{e-}(0) + W_i(\xi_0) - W_i(-\xi_{0-})), \\ \lim_{c_+\to\infty}[F^+ - F^-] &= 0 \end{aligned}$$

for all $x_0 > 0$. Since $F^+ - F^-$ is monotonic in c_+, then the only value of c_+ that satisfies the implicit equation is ∞. On the other hand, we have already shown that $c_+ \to \infty$ is not a solution of Eq. (3.18). Thus there could not have been a point at which $c_+ = |c_-|$ for any $x_0 > 0$. Hence, $c_+ > |c_-|$ for all $x_0 > 0$. This proves that the speed of the wave moving in the same direction as the stimulus is faster, as observed experimentally by Knapen et al. [13]. In Fig. 5B, we show a plot of the wave speeds versus x_0 calculated from our analytical expressions. Note that in the given parameter regime, the negative wave speed solution disappears at a critical value of x_0, as discussed at the end of Section 3. In Fig. 5A, we give an example of a fast (same stimulus direction) and a slow (opposite stimulus direction) traveling wavefront, which are generated by numerically simulating the full neural field model given by Eqs. (2.1) and (2.2). The network is taken to operate in the regime of slow synaptic depression ($\tau_s = 100$), so that the results of our adiabatic approximation hold. In particular, the slopes of the space–time plots are consistent with the analytically obtained wave speeds. The numerical simulations were implemented using a direct Euler scheme and the trapezoid rule.

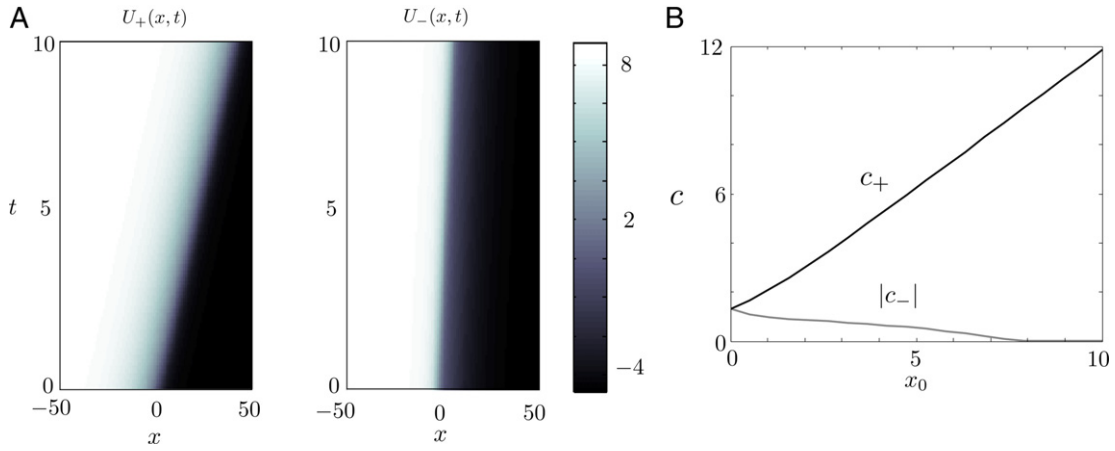

Fig. 5. Motion dependent wave speed. (A) Space–time plot of traveling fronts with positive wave speed (left) and negative wave speed (right) with $x_0 = 3$, obtained by numerically solving the full model given by Eqs. (2.1) and (2.2). Note that $U_-(x,t)$ has been reflected about the $x = 0$ axis for visual comparison against $U_+(x,t)$. (B) Plot of analytically obtained positive and negative wave speeds against x_0. Same parameter values were used as in Fig. 4.

5.2. Asymmetry in inhibition

We now analyze the dependence of wave speed on stimulus motion when we impose the asymmetry in the inhibitory weight function. Again, using the adiabatic approximation for the depression variables we can rewrite Eqs. (2.1) and (2.2) as

$$\begin{aligned}\frac{\partial u(x,t)}{\partial t} &= -u(x,t)+I_u \\ &\quad + Q_u\int_{-\infty}^{\infty} w_e(x-x')f(u(x',t))dx' \\ &\quad - Q_v\int_{-\infty}^{\infty} w_{i+}(x-x')f(v(x',t))dx', \end{aligned} \tag{5.12a}$$

$$\begin{aligned}\frac{\partial v(x,t)}{\partial t} &= -v(x,t)+I_v \\ &\quad + Q_v\int_{-\infty}^{\infty} w_e(x-x')f(v(x',t))dx' \\ &\quad - Q_u\int_{-\infty}^{\infty} w_{i-}(x-x')f(u(x',t))dx'. \end{aligned} \tag{5.12b}$$

In contrast to the previous analysis, $w_e(x)$ is a symmetric function while $w_{i\pm}(x) = w_i(x \mp x_0)$ is asymmetric, and $w_e(x)$ and $w_i(x)$ satisfy properties (i)–(iii) in Section 2. Without presenting the equations for the wave profiles we just look at the threshold conditions

$$\begin{aligned}\kappa &= Q_u W_e(0) - Q_v W_{i-}(\xi_0) \\ &\quad - \int_0^{\infty} e^{-\frac{\xi}{c_+}}\left[Q_u w_e(\xi) + Q_v w_{i+}(\xi-\xi_0)\right]d\xi \\ &\equiv F_1^+(c_+,x_0,\xi_0), \end{aligned} \tag{5.13a}$$

$$\begin{aligned}\kappa &= Q_v W_e(0) - Q_u W_{i-}(\xi_0) \\ &\quad + \int_0^{\infty} e^{-\frac{\xi}{c_+}}\left[Q_v w_e(\xi) + Q_u w_{i-}(\xi+\xi_0)\right]d\xi \\ &\equiv F_2^+(c_+,x_0,\xi_0). \end{aligned} \tag{5.13b}$$

Since

$$W_{i-}(\xi_0) = \int_{\xi_0}^{\infty} w_{i-}(x) = \int_0^{\infty} w_{i-}(x+\xi_0) \tag{5.14}$$

and

$$w_{i\pm}(x \mp \xi_0) = w_i(x \mp \xi_0 \mp x_0), \tag{5.15}$$

it follows that

$$\frac{\partial F_1^+}{\partial x_0} = \frac{\partial F_1^+}{\partial \xi_0}, \qquad \frac{\partial F_2^+}{\partial x_0} = \frac{\partial F_2^+}{\partial \xi_0}.$$

Therefore, from Eq. (5.1),

$$\frac{dc_+}{dx_0} = \frac{\frac{\partial F_1^+}{\partial \xi_0}\frac{\partial F_2^+}{\partial x_0} - \frac{\partial F_2^+}{\partial \xi_0}\frac{\partial F_1^+}{\partial x_0}}{\frac{\partial F_1^+}{\partial c_+}\frac{\partial F_2^+}{\partial \xi_0} - \frac{\partial F_2^+}{\partial c_+}\frac{\partial F_1^+}{\partial \xi_0}} = 0, \tag{5.16}$$

and thus the wave speed does not depend on stimulus motion. A similar argument holds for negative wave speeds.

6. Discussion

In this paper we explored direction selectivity in the context of binocular rivalry waves and analyzed the dependence of wave speed on stimulus motion. We used a continuum neural field model of competitive networks that has been used extensively in neural field literature to explain wave-like propagation in neural media [31]. We incorporated direction selectivity by imposing an asymmetry in the recurrent excitatory weight function involving a shift x_0 that depends on the speed of the stimulus; this was motivated by models of direction selectivity in cortical neurons. We showed that the speed of waves traveling in the direction of the stimulus increased as the stimulus speed increased. Additionally we found that, for a range of stimulus speeds, the speed of waves traveling against the stimulus decreased as the stimulus speed increased. Moreover, we showed that waves moving in the direction of the stimulus travel faster than waves in the opposite direction, consistent with the experimental and computational study of Knapen et al. [13]. It is important to note, however, that there are several major differences between our neural field model and the computational model of Knapen et al. [13]. First, the latter authors used spike frequency adaptation rather than synaptic depression as the slow negative feedback mechanism. Second, instead of including an asymmetric shift in the recurrent excitatory connections, they took the rate of spatial decay of the inhibitory weights to be asymmetric. Interestingly, we have shown analytically that, in the case of synaptic depression, an asymmetric shift in cross-inhibition does not generate differences in propagating and counter-propagating wave speeds. On the other hand, numerical simulations of our model (not shown) confirm that differences in wave speeds consistent with psychophysical experiments do occur when a spatial decay asymmetry is incorporated into the excitatory connections, but not when they are included in the cross-inhibition. Comparison with the computational model of Knapen et al. [13] thus suggests that the type of spatial symmetry breaking mechanism is sensitive to the form of slow adaptation.

However, certain caution must be exercised when making such a comparison, since we consider a 1D neural field, whereas Knapen et al. consider a ring network. From a mathematical perspective, a traveling wave only strictly exists in the former case, whereas on a ring or a finite interval a front-like solution is transient. It is not clear from the computational study of Knapen et al. whether or not there is sufficient time for front-like solutions to develop. Thus our mathematical analysis cannot be applied directly to their model on a ring. Nevertheless, one can view front solutions on an unbounded domain to be relevant to a bounded physical domain, under the assumption that the size of the domain is sufficiently large for a front-like solution to form. Therefore, it should be possible to extend the analytical methods presented in this paper to explore different combinations of weight asymmetries and adaptation processes in a more systematic fashion.

Another possible extension of our work would be to consider a more realistic two-dimensional network topology that can deal with more complex stimuli such as moving annuli. Instead of considering one line of neurons for each eye, we would introduce a circle of neurons for each point in the visual field — this would allow us to take orientation information into account using an extension of the coupled ring model [39,40]. We could then investigate the experimental observation that the speed of binocular rivalry waves also depends on the orientation of the patterns within the left and right eye annuli [5].

Acknowledgments

PCB was supported by National Science Foundation grant DMS-1120327 and SRC by the National Science Foundation grant RTG-1148230.

References

[1] P. De Weerd, R. Desimone, L.G. Ungerleider, Perceptual filling in: a parametric study, Vis. Res. 38 (1998) 2721–2734.
[2] N. Hadjikhani, M. Sanchez Del Rio, O. Wu, D. Schwartz, D. Bakker, et al., Mechanisms of migraine aura revealed by functional MRI in human visual cortex, Proc. Natl. Acad. Sci. USA 98 (2001) 4687–4692.
[3] J.M. Gold, E. Shubel, The spatiotemporal properties of visual completion measured by response classification, J. Vision 6 (2006) 356–365.
[4] D. Jancke, F. Chavane, S. Maaman, A. Grinvald, Imaging cortical correlates of illusion in early visual cortex, Nature 428 (2004) 423–426.
[5] H.R. Wilson, R. Blake, S.H. Lee, Dynamics of traveling waves in visual perception, Nature 412 (2001) 907–910.
[6] S.H. Lee, R. Blake, D.J. Heeger, Traveling waves of activity in primary visual cortex during binocular rivalry, Nature Neurosci. 8 (2005) 22–23.
[7] M. Kang, D.J. Heeger, R. Blake, Periodic perturbations producing phase-locked fluctuations in visual perception, J. Vision 9 (2009) 1–12.
[8] M. Kang, S.H. Lee, D.J. Heeger, R. Blake, Modulation of spatiotemporal dynamics of binocular rivalry by collinear facilitation and pattern-dependent adaptation, J. Vision 10 (2010) 1–15.
[9] P.C. Bressloff, M. Webber, Neural field model of binocular rivalry waves, J. Comput. Neurosci. 32 (2012) 233–252.
[10] M. Webber, P.C. Bressloff, The effects of noise on binocular rivalry waves: a stochastic neural field model: special issue on statistical physics and neuroscience, J. Stat. Mech. 3 (2013) P03001.
[11] R. Blake, A primer on binocular rivalry, including current controversies, Brain Mind 2 (2001) 5–38.
[12] R. Blake, N. Logothetis, Visual competition, Nature Rev. Neurosci. 3 (2002) 1–11.
[13] T. Knapen, R. van Ee, R. Blake, Stimulus motion propels traveling waves in binocular rivalry, PLoS One 8 (2007) e739.
[14] X. Xie, M.A. Giese, Nonlinear dynamics of direction-selective recurrent neural media, Phys. Rev. E 65 (2002) 051904.
[15] P.C. Bressloff, J. Wilkerson, Traveling pulses in a stochastic neural field model of direction selectivity, Front. Comput. Neurosci. 6 (2012) 90, 14 pages.
[16] H. Suarez, C. Koch, R. Douglas, Modeling direction selectivity of simple cells in striate visual cortex within the framework of the canonical microcircuit, J. Neurosci. 15 (1995) 6700–6719.
[17] R. Maex, G.A. Orban, Model circuit of spiking neurons generating directional selectivity in simple cells, J. Neurophysiol. 75 (1996) 1515–1545.
[18] L.C. Katz, C.D. Gilbert, T.N. Wiesel, Local circuits and ocular dominance columns in monkey striate cortex, J. Neurosci. 9 (1989) 1389–1399.
[19] D.H. Hubel, T.N. Wiesel, Receptive fields, binocular interaction and functional architecture in the cat's visual cortex, J. Physiol. 160 (1962) 106–154.
[20] G.G. Blasdel, Orientation selectivity, preference, and continuity in monkey striate cortex, J. Neurosci. 12 (1992) 3139–3161.
[21] D.H. Hubel, T.N. Wiesel, Functional architecture of macaque monkey visual cortex, Proc. R. Soc. Lond. B Biol. Sci. 198 (1977) 1–59.
[22] R.B. Tootell, E. Switkes, M.S. Silverman, S.L. Hamilton, Functional anatomy of macaque striate cortex. II. Retinotopic organization, J. Neurosci. 8 (1988) 1531–1568.
[23] R. Ben-Yishai, R.L. Bar-Or, H. Sompolinsky, Theory of orientation tuning in visual cortex, Proc. Natl. Acad. Sci. USA 92 (1995) 3844–3848.
[24] D. Ferster, K.D. Miller, Neural mechanisms of orientation selectivity in the visual cortex, Annu. Rev. Neurosci. 23 (2000) 441–471.
[25] L. Sincich, G.G. Blasdel, Oriented axon projections in primary visual cortex of the monkey, J. Neurosci. 21 (2001) 4416–4426.
[26] A. Angelucci, J.B. Levitt, E. Walton, J.M. Hupe, J. Bullier, J.S. Lund, Circuits for local and global signal integration in primary visual cortex, J. Neurosci. 22 (2002) 8633–8646.
[27] P. Sterzer, A. Kleinschmidt, G. Rees, The neural bases of multistable perception, Trends Cogn. Sci. 13 (2009) 310–318.
[28] D.H. Hubel, Single unit activity in striate cortex of unrestrained cats, J. Physiol. (Lond.) 147 (1959) 226–238.
[29] E.H. Adelson, J.R. Bergen, Spatiotemporal energy models for the perception of motion, J. Opt. Soc. Amer. A 2 (1985) 284–299.
[30] M.S. Livingstone, Mechanisms of direction selectivity in macaque V1, Neuron 20 (1998) 509–526.
[31] P.C. Bressloff, Spatiotemporal dynamics of continuum neural fields, J. Phys. A 45 (2012) 033001, 109 pp.
[32] Z.P. Kilpatrick, P.C. Bressloff, Binocular rivalry in a competitive neural network with synaptic depression, SIAM J. Appl. Dyn. Syst. 9 (2010) 1303–1347.
[33] A.L. Taylor, G.W. Cottrell, W.B. Kristan, Analysis of oscillations in a reciprocally inhibitory network with synaptic depression, Neural Comput. 14 (2002) 561–581.
[34] C.R. Laing, C.C. Chow, A spiking neuron model for binocular rivalry, J. Comput. Neurosci. 12 (2002) 39–53.
[35] A. Shpiro, R. Curtu, J. Rinzel, N. Rubin, Dynamical characteristics common to neuronal competition models, J. Neurophysiol. 97 (2007) 462–473.
[36] L. Zhang, On stability of traveling wave solutions in synaptically coupled neuronal networks, Differential Integral Equations 16 (2003) 513–536.
[37] S. Coombes, M.R. Owen, Evans functions for integral neural field equations with Heaviside firing rate function, SIAM J. Appl. Dyn. Syst. 3 (2004) 574–600.
[38] B. Sandstede, Evans functions and nonlinear stability of traveling waves in neuronal network models, Int. J. Bifurcation Chaos 17 (2007) 2693–2704.
[39] P.C. Bressloff, J.D. Cowan, M. Golubitsky, P.J. Thomas, M. Wiener, Geometric visual hallucinations, Euclidean symmetry and the functional architecture of striate cortex, Philos. Trans. R. Soc. B 40 (2001) 299–330.
[40] P.C. Bressloff, J.D. Cowan, An amplitude equation approach to contextual effects in visual cortex, Neural Comput. 14 (2002) 493–525.